

COLLOID CHEMISTRY
AND ELECTROCHEMISTRY

Effect of Experimental Variables on the Physicochemical
Characteristics of Multi-Responsive Cellulose
Based Polymer Microgels

Abbas Khan^{a,*}, Uzma Rehmat^a, Luqman Ali Shah^b, and Muhammad Usman^c

^aDepartment of Chemistry, Abdul Wali Khan University Mardan, 23200 Pakistan

^bNational Centre of Excellence in Physical Chemistry, University of Peshawar, 25120 Pakistan

^cDepartment of Chemistry, Government College University, Faisalabad, 38000 Pakistan

*e-mail: abbas053@gmail.com, abbas80@awkum.edu.pk

Received September 25, 2019; revised September 25, 2019; accepted October 15, 2019

Abstract—Temperature and pH responsive macromolecular colloidal materials have widespread applications. pH/thermo-responsive benzyl modified cellulose based microgels (BMC-PNIPAAm-PAAc) were synthesized by copolymerization of benzyl modified cellulose with poly(N-isopropylacrylamide) [PNIPAAm], and acrylic acid (AAc) by emulsion polymerization. In order to enhance the copolymerization ability of cellulose, its hydroxyl groups were modified by treating with benzyl chloride. Microgels were characterized using Fourier transform infrared spectroscopy (FTIR), UV–Vis spectroscopy, rheology, dynamic light scattering (DLS), flow viscometry, and density measurements. FTIR was used to investigate the various functional groups in the microgels. The influence of experimental conditions such as chemical composition and temperature/pH of microgel solutions on the sol–gel behavior of microgels was studied through rheology, light scattering, viscometry and densimetry. The shear stress and gel viscosity was measured under various shear rates and temperatures. By increasing the shear rate, a decrease in viscosity was observed. The microgels behaved as viscoelastic solids over a wide frequency range as the loss modulus was found to be smaller than the storage modulus. Temperature-dependent spectral changes of the microgels were also investigated by UV–Vis spectroscopy at various temperatures. The relative viscosity of the synthesized microgels was also studied at various pH/temperature using concentration based times of flow Ostwald’s viscometry. Similarly, the specific volume of the gel particles was traced from the solution density. The results revealed that various colloidal and physicochemical parameters of the polymer gels could be easily adjusted by changing various experimental variables, suggesting their potential use as drug delivery carriers.

Keywords: cellulose, microgel, swelling, light scattering, viscosity, rheology

DOI: 10.1134/S003602442007016X

INTRODUCTION

Polymer microgels have been paid attention in fundamental studies of colloid science and for use in widespread applied fields over the past few years. As is well known, they have extensive important applications in material science because of their three dimensional network cross-linked colloidal gel particle structures [1]. For biomedical applications, stimuli-responsive hydrogels of biopolymers have been considered as biopolymers because of high content of their functional groups, superb biodegradability, low toxicity, and biocompatibility [2, 3]. Natural polysaccharides, like hyaluronic acid, alginate, chitin, chitosan, and dextran are commonly available biopolymers. Due to their biocompatibility and biodegradability, they have been used for biomedical applications [4, 5]. Significant interest has been shown in these stimuli-responsive polymer microgels because of their pro-

spective applications in chemical sensors [6], drug delivery [2], catalysis [7], optical devices [8], tissue engineering [9], and pollution control [10]. This has led to the preparation of novel microgels with enhanced response upon stimuli application such as solvent polarity [11], light irradiation [12], electrical fields, pH [13], ionic strength [14] and some specific chemicals which have structural resemblance with them. It has been noticed that microgels prepared from natural polymers like cellulose, starch, gelatin, alginate and chitosan, have been used to deliver a large variety of therapeutics, such as antibodies, hormones, antibacterial compounds, contraceptives, enzymes and vaccines. The most abundant natural resource in the universe is cellulose, which has been selected as a promising material for fabricating microgels due to its biodegradability, hydrophilicity and safety [15].

Natural anhydro-glucose monomer (with 1-4 β linkages) is the fundamental unit of a linear chain cel- lulosic polymer with the terminal-ends having reduc- ing and non-reducing sugar units that stabilize the cel- lulose polymer. The chemical and physical properties of cellulose can be ascribed to reactive OH groups that occupy one of the three positions, C-2, C-3, and C-6. The polymer chain is tightly and compactly arranged due to the presence of various interactive force i.e., strong intramolecular H bonding, intermolecular forces, and weaker Van der Waals forces [16]. The attention of technologists and scientists is on the nat- ural fibers reinforced composites has increasing, this is due to their prospective use as substitutes for use as fillers in artificial fiber composites [17, 18]. To improve this class of materials with better stimuli responsivity and biodegradability, we propose that the development of benzyl modified cellulose based microgels (BMC-PNIPAAm-PAA particles with both thermo- and pH sensitivity simultaneously would be useful. However, there is the need to address the insuf- ficiency of information on the fundamental physico- chemical properties of these copolymer microgels. In particular, to better understand the fundamentals of this cellulose-based responsive material, one has to understand in detail the effect of several internal and external parameters on its physicochemical properties.

Stimuli-responsive hydrogel systems have been based on interpenetrating polymeric networks (IPNs) [19]. Poly(N-isopropylacrylamide) (PNIPAAm) is a most common and well-known source of thermo- responsive polymeric networks in the set of stimuli- responsive polymers. In aqueous medium that are responsive, it has a coil-to-globule transition at around 32°C [20]. A reversible transition phase occurs which induced by a change of temperature about its LCST (lower critical solution temperature) \approx 32°C. At low temperature PNIPAAm is water soluble but at high temperature it phase separates. It has outstanding capabilities as a biologically active molecule for use as a protective container and potential carriers for drugs [21]. However, it was noticed that when changing the temperature PNIPAAm show low response rate as a result of a dense skin layer which slows down the out- ward diffusion of water molecules during the hydrogel collapse above the LCST [22]. Polymer microgels with better responses to numerous stimuli are very import- ant from application point of view. Previously, we have worked on chitosan-PNIPAAm based responsive microgels, Their physicochemical behavior was stud- ied under various pH and temperature condition and it was seen that this microgel system has good response to temperature and pH of the medium. However, it was concluded that their multi-responsive behavior, especially pH-responsive ability, could be improved by the incorporation of carboxylic acid into their structure [23]. Thus, to get multi-responsive micro- gels, we copolymerize PNIPAAm with an ionic monomer containing carboxylic acid groups to form

pH and temperature sensitive microgels. We propose that the combination of acrylic acid (AAc), poly(N- isopropylacrylamide), and a biopolymer (Cellulose) resulted in a new material with an enhanced volume phase transition (VPTT) and biodegradable proper- ties, which could have better biomedical applications compared to any of their homopolymer alone. The polyelectrolytes, having weak acidic and basic groups in their structure, can accept or release protons in response to changes in the environment pH. They can undergo ionization similar to monoacids and mono- bases. On the other hand complete ionization is more difficult on polyelectrolytes due to electrostatic effects which are exerted by neighboring ionizable groups [24, 25]. Therefore, it is important to produce a terpolymer gel with thermo-, pH, and biodegradable properties. The present report describes a one-pot synthesis and detailed physicochemical investigation of the Cellu- lose-PNIPAAm-PAAc microgels with good thermo-, pH, and biodegradable properties.

EXPERIMENTAL

Materials

All chemicals used in this project, except cellulose, were purchased from Sigma-Aldrich United States. These include acetone, NaOH, dilute acetic acid, benzyl chloride, ethanol, dimethylacetamide (DMA), anhydrous LiCl, cellulose, NIPAM, acrylic acid (AAc), methylene bisacrylamide (MBA), ammonium persulfate (APS), dilute HCl solution, and trypan blue. Cellulose was extracted from the branches of *Wikstroemia canescens* Meisn., collected from the local area of district Buner in Pakistan.

Extraction, Modification, and Dissolution of Cellulose

For the preparation of the copolymer microgel, cellulose was extracted from the branches of *Wikstro- emia canescens*. These plant branches were first soaked in water for 40 days; the fibers were separated from the sticks by hands and washed with a detergent solution. These fibers were dried in a drying oven for 24 h at temperature of 70°C and further subjected to Soxhlet extraction for 72 h with acetone and then washed with distilled water twice and air dried. The extracted cellu- lose threads were then modified using a benzylation approach as summarized here. The cellulose fibers were pretreated for 4 h in a 10% (w/v) NaOH solution to activate the hydroxyl groups of cellulose. The result- ing fibers were then washed with distilled water to remove the NaOH and in a 2% (w/v) dilute acetic acid solution (250 mL) to neutralize the fibers and again washed with distilled water. At room temperature these fibers were dried for 2 days followed by hot air drying at 70°C. One gram of pre-treated fibers were then suspended in 100 mL of 10% NaOH solution and shaken well with various concentrations (1, 2, 3, 5, 7, and 9%) of benzyl chloride for 10–15 min each, fil-

Table 1. Chemical composition of monomer, comonomer, and cross-linker in microgel samples

Sample code	BMC, mL	AA, mL	NIPAAm, g	MBA (cross-linker), g	APS (initiator, 0.8 M), mL	Total volume, mL
USG1/S1	30	5.0	0.5	0.02	15	100
USG2/S2	30	10	0.5	0.02	15	100
USG3/S3	30	10	1	0.02	15	100

tered and then finally washed thoroughly with distilled water and dried in the folds of filter papers. The isolated fibers were then soaked in ethanol for 60 min to eliminate unreacted benzyl chloride and then washed with water and finally dried [26]. For dissolution of the benzyl modified cellulose (BMC), 1 g of BC fibers, and 40 mL of DMA were kept in a three neck conical flask at 130°C under stirring for 2 h. The mixture was allowed to cool to 100°C. After this, three grams of anhydrous LiCl were added to the slurry. The cellulose fibers were dissolved completely in water on cooling to room temperature under stirring [27].

Synthesis of the Microgel Samples

After the extraction and dissolution of the benzyl modified cellulose (BMC), the copolymer microgel was synthesized through the free radical copolymerization of BC, NIPAM, and acrylic acid (AAc). In a three neck flask, a proper amount of NIPAM, cellulose, AA, and cross-linker (MBA), were dissolved in 100 mL of distilled water (for composition, Table 1) and a few drops of acetic acid were added to it. The reaction flask was equipped with an inlet of inert gas (N₂) system and condenser. To create active sites in the cellulose chains, the reaction mixture was stirred with a constant speed at 30°C for 24 h in the presence of acetic acid [28]. After 24 h, the temperature was raised up to 70–75°C and then to start the free-radical copolymerization reaction under constant temperature and inert condition, 5 mL of APS (0.8 M) solution were added to the reaction flask. After a few minutes appearance of the reaction mixture turned to milky and for completion of the copolymerization process the reaction was allowed to continue for 5–6 h. In order to purify the resulting microgel, the dialysis was performed against the regular changes of dilute HCl solutions in water with pH values set by 5 ± 0.3 at room temperature (25°C) for one week followed by filtration and drying in the folds of filter paper at ambient temperature. Furthermore, the samples were

characterized with the help of UV–Vis and FTIR spectroscopy, laser light scattering, rheology, density, and viscosity measurements.

Characterization of Microgels

A summary of the physicochemical characterization of the gels is given here.

FTIR. Fourier transform infrared spectroscopy (FTIR) was used to obtain the IR spectra for chemical composition of oven dried BMC-PNIPAM-PAA microgel samples. The range of wave number was from 500–4000 cm⁻¹ while using an IRAffinity-1S model IR-spectrometer (Shimadzu Ltd., Japan).

Rheology. The oscillatory and steady shear rheological measurements were accomplished with “MCR 301 (Anton Paar Ltd., Austria) with parallel plate geometry and the distance between plates was 1 mm. This instrument uses the measuring plate PP25/PE diameter: 25 mm material: stainless steel/PEEK PP25 system. The temperature range was 20–60°C while the frequency range for the oscillatory shear measurements was 0.001–100 rad/s. The computer software was used to obtain the rheological parameters, such as viscous modulus, G'' ; elastic modulus, G' ; and complex viscosity, η^* .

UV–Vis spectroscopy. A double beam Lambda 50 UV–Vis spectrophotometer (Perkin Elmer Ltd., USA) was used to determine the UV/Vis absorption spectrum of different composition of microgels with quartz cuvettes having 1 cm optical path length.

Light scattering. Dynamic light scattering (DLS) measurements for size determination were performed on a standard Malvern NANO ZS Zetasizer (Malvern Instruments Ltd., UK), using a He–Ne laser with a wavelength of 633 nm, and a detector angle of 90°. All microgel solutions were passed through Millipore Millex-HV filters (with a pore size of 0.80 μm) to remove dust before the DLS measurements. All solutions were equilibrated at each chosen temperature/pH for 15 min before the reading.

Density and viscosity. Different percent solutions (5, 10, 15, 20, 25, and 30%) were prepared. To measure density, a 25 mL specific gravity bottle was calibrated by using deionized water. The samples were filled in the specific gravity bottle and the densities of

Table 2. FTIR peaks (cm^{-1}) of prominent functional groups detected in BMC-PNIPAAm-PAA microgels for USG1 (I), USG1 (II), and USG1 (III)

Group	I	II	III
N–H (stret)	3317	3317	3317
C–O	1017	1017	1017
C–C	1600	1600	1600
O–H	1400	1400	1400
C–N	1267	1267	1267

samples were noted. The viscosities of the samples were measured at various temperatures in the range 20–60°C using a flow method.

RESULTS AND DISCUSSION

FTIR Study

BMC-PNIPAAm-PAAc based gels were tested with FTIR for their chemical composition and confir-

mation of microgels formation. Absorption peaks at various positions were recorded in the spectra of three the samples and the summary of their positions/identification is given in Table 2. A broad band at approximately 3400 to 3317 cm^{-1} was assigned to the stretching vibrations of N–H groups of MBA. The peak at 1017 cm^{-1} is due to the C–O stretching vibrations. The carbon–carbon double bond absorption band at 1600 cm^{-1} while the absorption peak at 1267 cm^{-1} is associated with C–N stretching vibrations of the amino group of primary amines [23]. The typical absorption peak of OH groups of both the carboxylic acid and NIPAAm are shifted to 1400 cm^{-1} which is an indication of the polymerization of both monomers. Likewise, the typical absorption peaks at 800–1000 and 1460 cm^{-1} , which generally appeared in the NIPAAm spectrum, were not observed which is again an indication that polymerization had taken place. On the basis of overall results, a physical structure of the microgel was proposed as shown in Fig. 1.

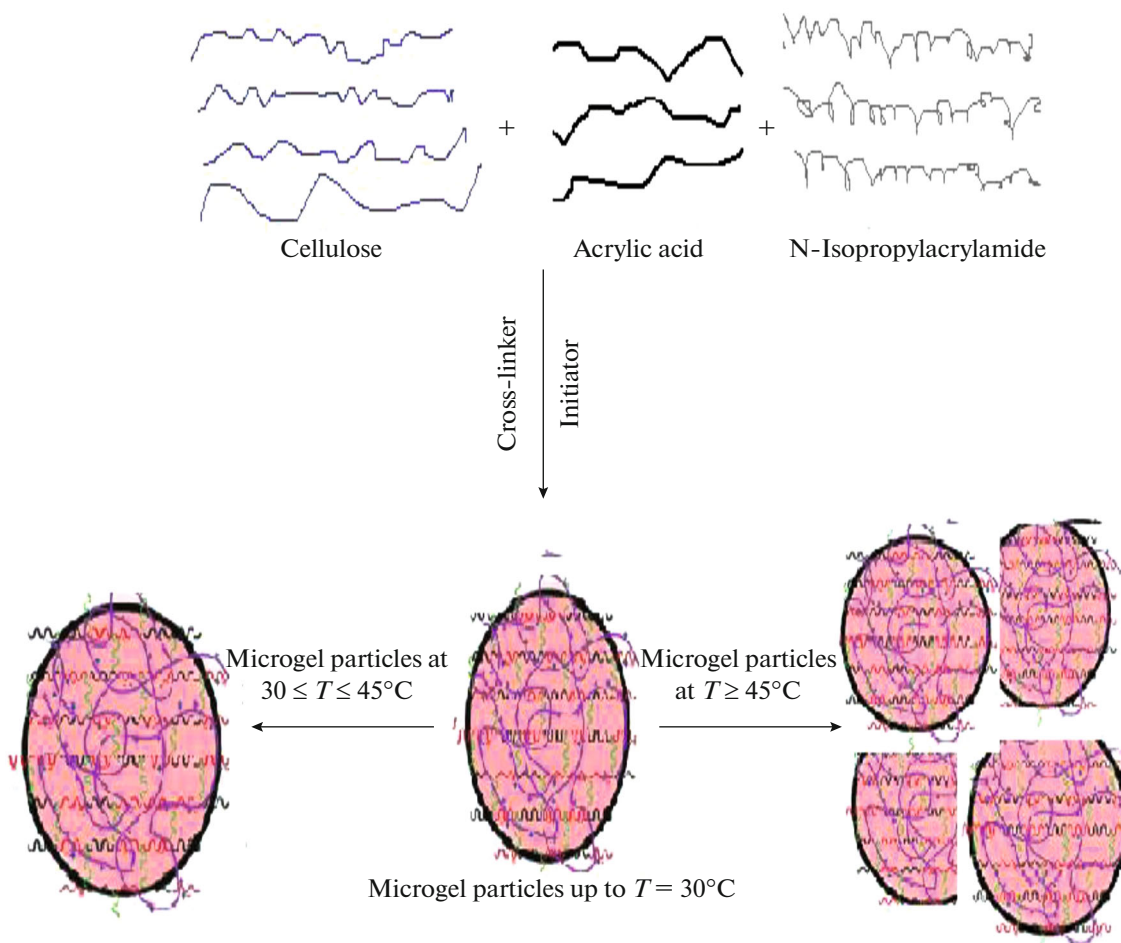


Fig. 1. (Color online) Proposed mechanism and possible physical structure of BMC-PNIPAAm-PAAc microgels.

UV–Vis Study

In order to get more information regarding the synthesis of the polymer gel and to check the temperature sensitivity, UV–Vis spectral behavior of the gel was investigated at various temperatures from 20 to 60°C. It was seen that original microgel solution did not show any peak in the visible region (350–800 nm) which means that microgels are entirely saturated, as shown in our previous work [23]. Unsaturation was not found in the structure of microgels. Then the microgel was mixed with a 20% trypan blue solution and measurements were made, which resulted in obtaining an absorption band in visible region of the spectrum. Figure 2 reflected the change in the shape, height and position of the dye peak in the presence of the microgel while changing the temperature of the solution. This suggests that the microgel showed a physicochemical type interaction with trypan blue, whose strength is altered by changing the experimental temperature. Further, sample 3 with larger amount of NIPAAm in its feed composition showed different temperature-sensitive physicochemical behavior toward dye as compared to other two samples.

Rheological Studies

Viscosity versus shear rates. The rheological study of thermo- and pH-responsive microgels in aqueous medium is useful to elucidate the association behavior and phase changes at different temperatures and pH in response to shear rate [29]. The viscosity-shear rate profiles for samples USG1, USG2, and USG3 at the same temperature is shown in Fig. 3, while more details of viscosity variation with shear rates under varying experimental temperature for sample 2 can be inspected from Fig. 4. An overall study of the figures shows that the shear rate had a contrary relationship with viscosity; as the microgel become thinner with increasing shear rate as the viscosity of gel decreased at all temperatures due to shear based thinning behavior, and a sort of pseudo plasticity was found in the gels. The comparison between the viscosities of USG1, USG2, and USG3 at 35°C (Fig. 3) shows that the viscosity at any given shear rate was in the order USG2 > USG3 > USG1; we attribute this to the different NIPAAm/AAC ratios in their composition (Table 1), USG2 having higher ratio of AAC/NIPAAm than the other two. This effect altered the hydrophilic/hydrophobic ratio of microgel sample above the lower critical solution temperature (LCST \approx 32°C) of NIPAAm; at higher NIPAAm/AAC ratio the gel become more hydrophilic-hydrophobic interactions was changing, and consequently, the gel became more compact.

Regarding the effect of temperature on the viscosity-shear rate profile, it is seen that all sample showed temperature sensitivity as can be seen from the changes in Y-axis of a representative figure for sample 2 (Fig. 4). The temperature dependence of the

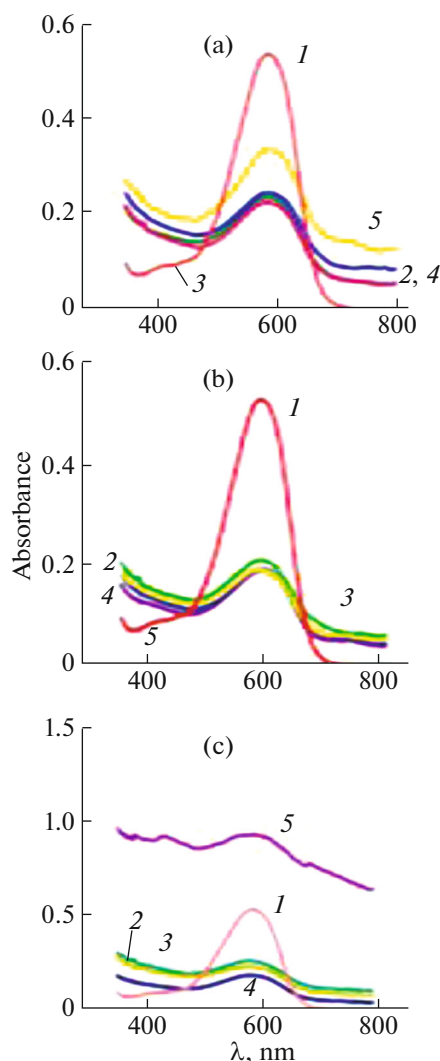


Fig. 2. (Color online) Effect of temperature on the UV–Vis spectra of trypan blue in the presence of microgel samples: (a) 1, (b) 2, (c) 3; $T = 20$ (1), 30 (2), 40 (3), 50 (4), and 60°C (5).

viscosity of USG1 shows two main phenomena. A large decrease in viscosity was observed, up to 30°C because the hydrophilicity of the gel enhances with temperature in this range due to the presences of NIPAAm, however, after reaching a certain temperature called volume phase transition temperature (VPTT), a gradual increase in viscosity was observed [29]. This increase in viscosity was due to dehydration and shear thickening property of hydrogel. Sample USG2 showed different behavior compared to USG1 because of different composition. In USG2 the concentration of AAC was greater than in USG1, so the viscosity of USG2 was different. In the temperature 20–30°C USG2 showed a decrease in viscosity; as strong interaction between water molecules and gel particles were observed due to upper critical solution temperature (UCST) of AAC and the gel becomes

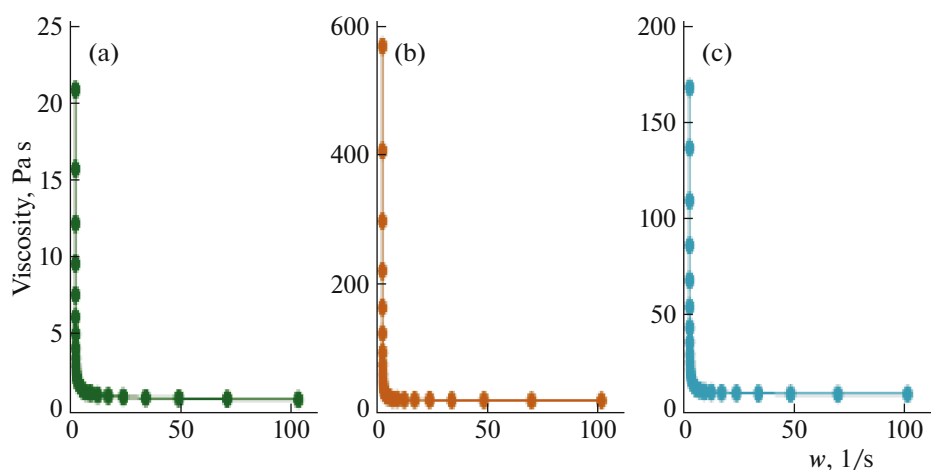


Fig. 3. (Color online) Viscosity versus shear rate (w) at 35°C for (a) USG1, (b) USG2, and (c) USG3.

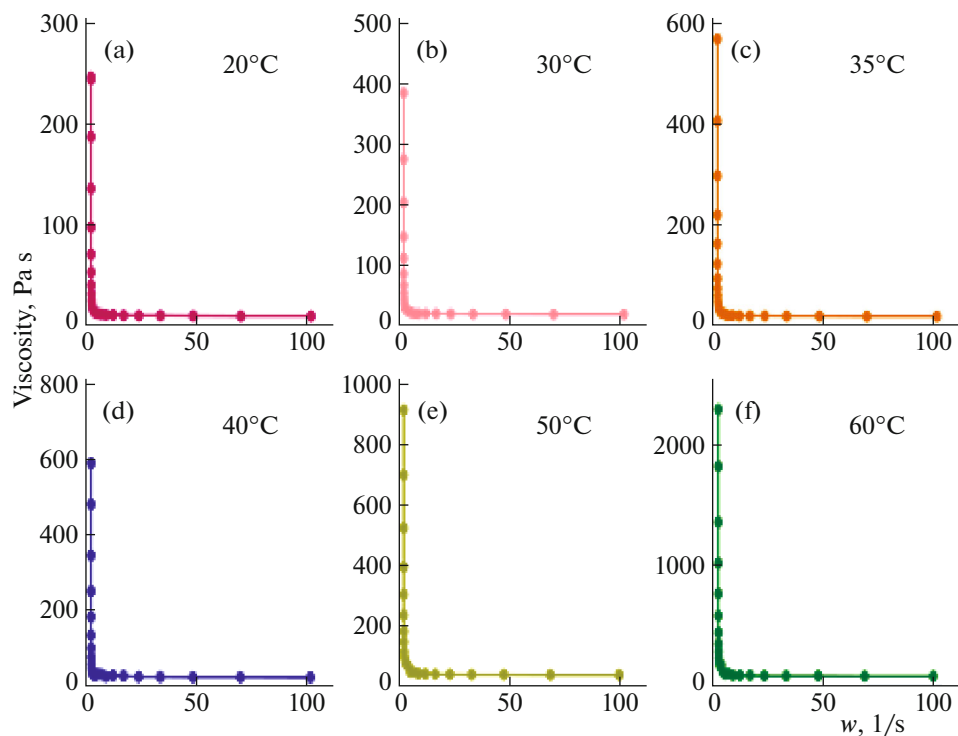


Fig. 4. (Color online) Viscosity versus shear rates (w) profiles of sample 2 (USG2), at different temperatures.

thinner [30]. With increasing the temperature from 30 to 60°C the viscosity of the hydrogel continued to increase, the gel became hydrophobic, lost water and the gel–gel interaction were greater as compare to the gel–water interaction due to hydrophobicity of NIPAAm and the gel particles became harder [31]. For sample 3 (USG3) the concentration of NIPAAm was greater while the concentration of AAc was the same as that in USG2. As for sample the viscosity of USG3 first decreased from 20 to 30°C. This decrease

in viscosity was due to gel–water interactions while above LCST gradual increases in viscosity was observed [32]. Above the LCST of NIPAAm the swollen particles shrank due to disruption of hydrogen bonding with water molecules and also the hydrophobicity of NIPAAm.

The shear stress versus shear rates study. Almost linear relationship was observed between shear stress and shear rates for all samples. A representative figure for shear stress–shear rate profile for sample 1 (USG1)

at different temperature is given in Fig. 5. In USG1 the amount of AAc was low, so the size of gel particles was small and more shear stress was required to change the phase of the gel particles [27]. As the temperature was increased from 20 to 30°C, the shear stress decreases due to the hydrophilic character of NIPAAm while with further increasing temperature (above 30°C), the shear stress required for any shear rate also increased and then remained constant at higher temperature; this was due to the variation in hydrophilic/hydrophobic balance and hence the shear thickening of the microgel at high shear stresses. The water was expelled from the gel with increasing temperature from 35 to 40°C and the gel became rigid and greater force is required for its deformation. In USG2 the concentration of AAc was greater than in USG1, so, more shear stress is required for USG2 at nearly all temperatures as compared to sample 1. At 30°C the gel particles became less viscous due to the absorption of water and the size of the gel was increased, so, less shear stress was required for the less viscous samples to deform the microgels. At temperature above 30°C the hydrophobic character of NIPAAm was increased, the sample become more viscous so the gel underwent deformation by applying more shear stress than low temperature [33]. The stress-strain profile also dropped above 40°C; this was assigned to the aggregation of gel particles and hence less stress could be enough for deformation of the aggregate compared to a single gel particle. For USG3 the graphs indicate that with increasing temperature, up to 30°C a decrease in shear stress was observed due to looser structure of the gel [34]. This shows that stronger gel–water interaction occurred instead of gel–gel interaction and hence less shear stress was needed to deform the microgels. At temperature, greater than 30°C this gel showed almost similar behavior as that of USG2. A comparison among USG1, USG2, and USG3 at single temperature reflected that USG1 had a lower shear stress value than USG2 and USG3 due to the lower amount of AAc. However, by comparing USG2 and USG3 it was observed that USG2 needed relatively higher shear stress value for a given shear rate as compared to USG3; his maximum value of shear stress of USG2 is due to the larger amount of AAc and due to this the cross-linker effect is also dominant. The size of particles was smaller for this sample (DLS results), therefore can easily bypass each others during flow.

The study of storage and loss moduli versus angular frequency. The effect of temperature on the storage and loss moduli as a function of angular frequency for a representative sample USG2 (sample 2) is shown in Fig. 6. It is important to recall here that on the basis of their viscoelastic behavior, polymeric samples can be divided into viscoelastic solids, gels and liquids. Normally, the storage modulus represents the elastic component of the material while the loss modulus denotes the viscous behavior of the samples. In the present

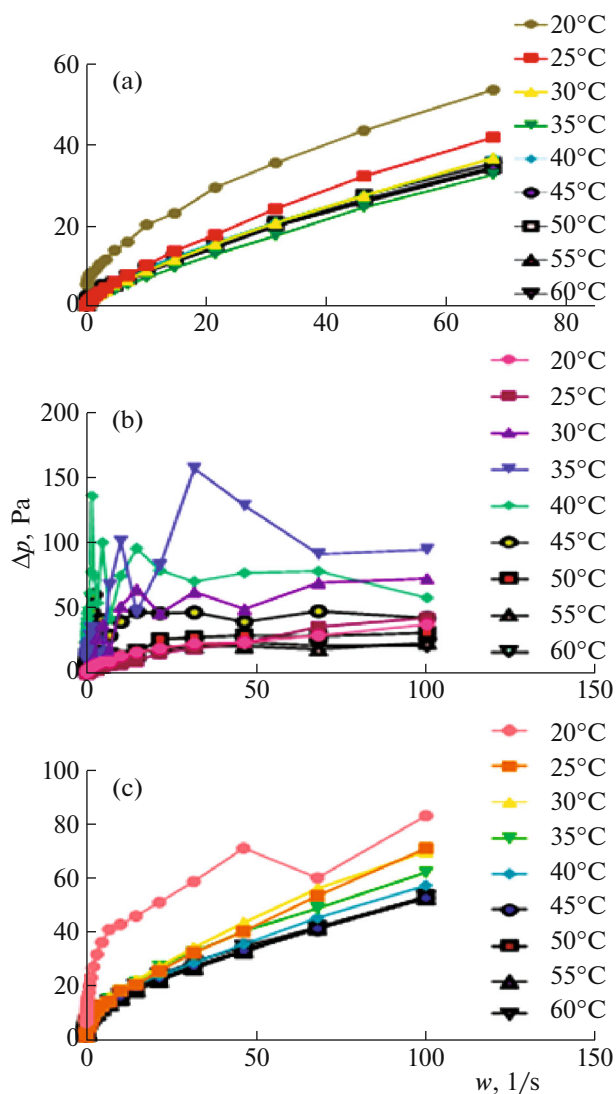


Fig. 5. (Color online) Shear stress (Δp) versus shear rates (w) at various temperatures for (a) USG1, (b) USG2, and (c) USG3.

study it was seen that both of these moduli versus angular frequency (ω) varied almost linearly with increasing ω . Also the moduli have different values/behaviors at different temperatures for all samples. It was seen that the storage modulus (G') was greater around the LCST (35°C) of NIPAAm, this showed that the gels are more elastic and less viscous under these conditions and the gel showed a higher degree of internal structure and hence more stable in solution. At higher temperatures the storage modulus (G') was relatively smaller, which suggested that the gel became more viscous and lost its elastic character by expelling water from the gel. This lesser storage modulus (G') indicates that the individual size (not of aggregates) of the gel particle may be smaller except sample 3 which had higher NIPAAm in its composition [35]. However, aggregation of the particles will

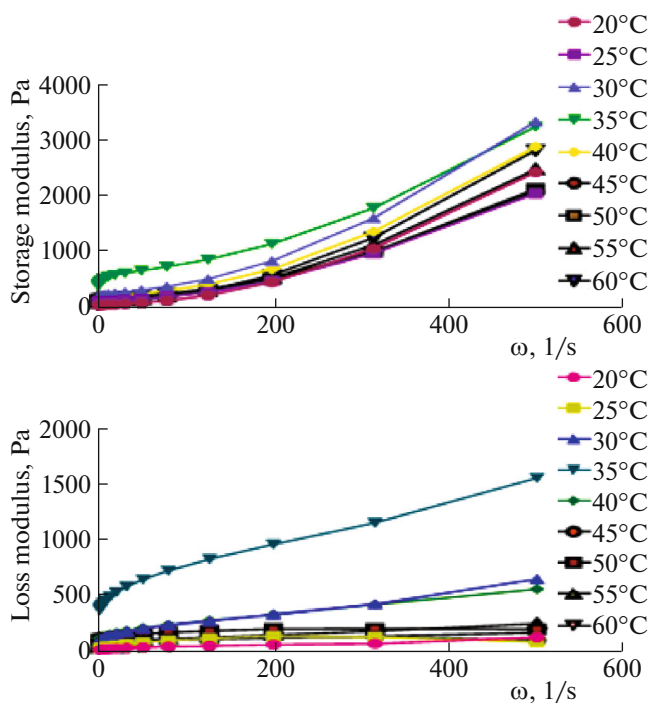


Fig. 6. (Color online) Typical figure showing the effect of temperature on the moduli as a function of angular frequency (ω) for representative sample USG2.

increase the average size producing fewer particles of the bigger size due to more solute–solute interaction. Above the LCST the gel became less elastic and more viscous due to hydrophobic character of NIPAAm and less storage modulus (G') was needed at any given angular frequency [29]. The concentration of NIPAAm in USG3 was greater than USG2. For USG3, with increasing temperature above the LCST of NIPAAm the gels showed a decrease in storage modulus (G') significantly [31]. This showed that above LCST chains of the NIPAAm were collapsed and that significantly modified the elastic behavior of gel. The comparison of various samples at the same temperature (30°C) showed that the value of storage modulus (G') was higher for USG2 which as attributed to higher AAc ratio in this sample.

The loss modulus (G'') of the gels also varied with the changes in chemical composition and temperatures. It was observed that G'' was smaller below the volume phase transition temperature while it increased with temperature and then decreased again. This fluctuation in loss modulus (G'') was attributed to the hydration/dehydration of water from the gels with temperature. As the temperature increased the gels transfer from hydrophilic to hydrophobic state and an increase in loss modulus (G'') was observed [35]. Increase in loss modulus (G'') was also observed in USG2 at lower temperatures due to its smaller particle size, as confirmed by DLS results. These gel became hydrophobic at temperatures greater than 30°C which

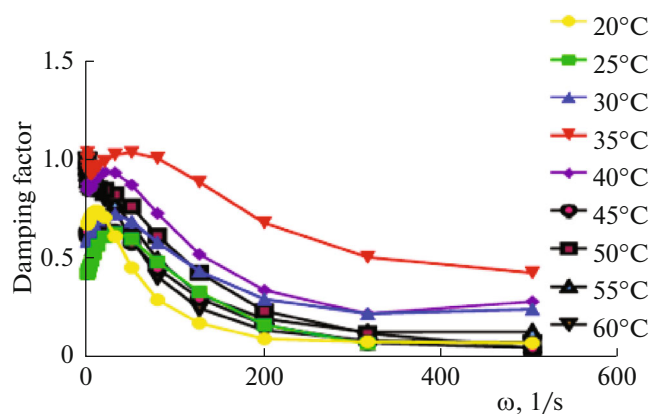


Fig. 7. (Color online) Damping factor versus angular frequency at various temperatures for USG2.

pump out water due to the hydrogen bond formation between $-\text{COOH}$ groups of the gel particles [36]. The value of the loss modulus (G'') decreased further above the LCST of NIPAAm due to the hydrophobicity. In case of USG3, a decrease in loss modulus (G'') is observed from temperature 20–30°C this is due to the interaction between gel and water molecule, as this gel has a relatively higher concentration of NIPAAm. But at temperature above 30°C, the loss modulus (G'') increased again [36]. Among these samples the value of the loss modulus (G'') is high in USG2 (higher AAc amount) due to more solute–solvent interactions.

Effect of angular frequency on the damping factor of the gels. The damping factor is the ratio between loss modulus (G'') and storage modulus (G') or $(G''/G') = \tan d$. The ratio of the moduli (G''/G') usually indicates the relative degree of energy dissipation or damping of the material. The communication of the internal morphology is studied by damping factor. A collaboration between the gel particles depend upon the value of G'' the larger the G'' value (smaller the $\tan d$), so greater will be the communication between the gel. Viscoelasticity of the microgels was explained also by plotting the graphs between loss factor and angular frequency. The variation of damping factor with angular frequency for sample USG2 at different temperature can be seen in Fig. 7. The values of $\tan d$ were lower than one at almost all frequencies for all samples indicated that the elastic component of the gels was dominant than their viscous component. As the loss factor further decreased with increasing the frequency which suggested that the elasticity enhanced at higher frequencies. Results also indicated that values of the damping factor decreased with the passage of time and increases with temperature up to VPTT.

The study of complex viscosity versus angular frequency. The study of complex viscosity of the microgels as a function of angular frequency over a wide range of temperature could give more information about the extent to which the gel behave as solid or liq-

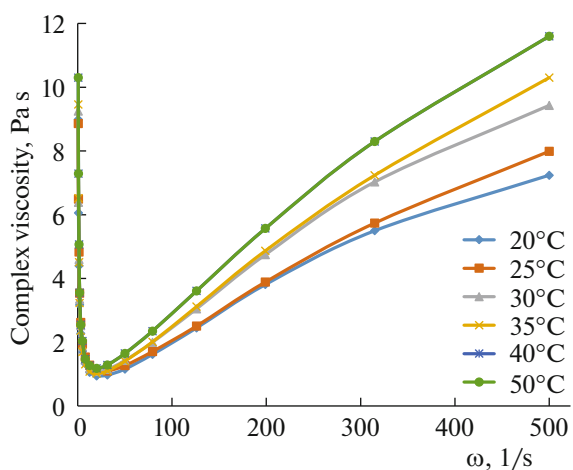


Fig. 8. (Color online) Complex viscosity versus angular frequency at various temperatures for USG1.

fluid like [37]. The graphs of complex viscosity (η^*) versus angular frequency (ω) for USG1 at different temperatures are shown in Fig. 8. It was found that complex viscosity (η^*) decreased with angular frequency (ω) in the lower frequency region and then increased with frequency at all temperatures. This reduction in the complex viscosities was due to abating of the cross-linking density. At higher angular frequencies all curves were congregating for various temperature indicated a solid-like behavior of the gels. The changes in complex viscosity with temperature reflected the temperature dependent changes in the internal structure of the gel (sol–gel transition) [38]. The increase in complex viscosity with temperature supported the idea that molecular motion became passive due to shear thickening effect; under these conditions the free space available for the polymer chains movement decreased. This in turns increased the intra- and intermolecular resistive forces associated with thicknesses/viscosity of the microgel particles. Rheological results confirmed the temperature sensitivity and temperature based volume phase transitional changes of the gels.

Light Scattering Analysis

Dynamic light scattering measurements were carried out to collect more knowledge about the temperature/pH depending swelling/de-swelling behavior of the gel samples [39]. Figure 9 gave information about the dependence of hydrodynamic diameter (D_h) on temperature and pH of the medium for all samples. An analogous changes in the D_h –temperature and D_h –pH profiles were observed samples 1 and 2 while sample 3, which had higher NIPAAm as compared to other two (Table 1) got comparatively larger size, this was due to formation of the longer polymer chain for this sample. The D_h –temperature profiles showed that volume

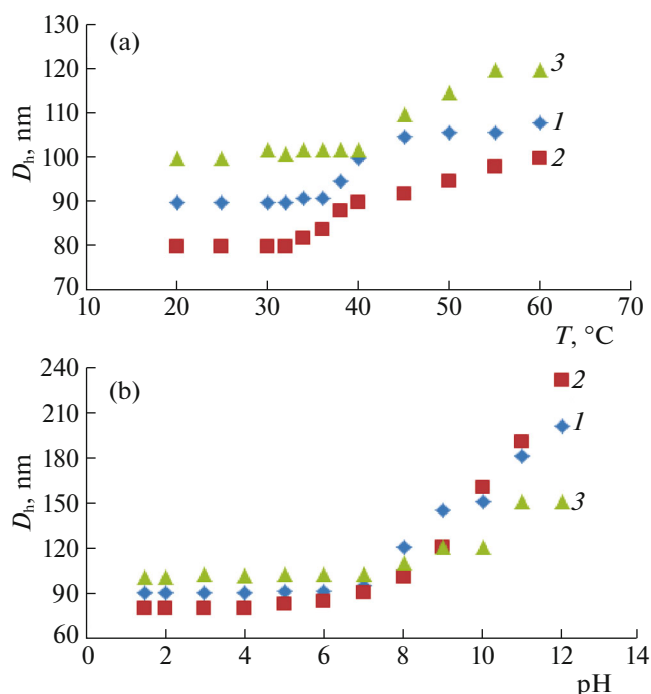


Fig. 9. (Color online) Variation of the hydrodynamic diameter as function of (a) temperature at pH 5 and (b) pH of the gels solution at 30°C (concentration 10%), (1) USG1, (2) USG2, and (3) USG3.

phase changes occurred in three steps. In the first step (20–35°C) the D_h values remained constant while in the second region (35–45°C) size of microgels increased with temperature. This increase in size is due to volume phase changes in the gel due to the presence of NIPAM moiety which was discussed in detail in rheological results. In the third region ($T > 45^\circ\text{C}$), the microgel size changed less prominently; the effect was attributed to compensation of increase in size due to aggregation by dehydration (de-swelling) at higher temperature. The variation of size in response to pH (D_h –pH graphs) was divided into three sections as well. When $\text{pH} \leq 5$ values D_h remained constant while from pH 5–8 a minor increase in size was seen; however, at $\text{pH} > 8$ a prominent increase in particle size was observed. These changes in D_h with pH were assigned to the presence of acrylic acid (AAc) in composition of the gel and hence to its protonation–deprotonation in response to pH. At pH above the pK_a value of AAc the ionization of the gel (AAc) could occur, which developed some negative charges on the chains of gel particles. These charged particles might repel each other and created more spaces (free volume) for water molecules to go inside and turned the molecules more hydrophilic. These changes resulted in an increase in particle size. The final prominent increase in size of

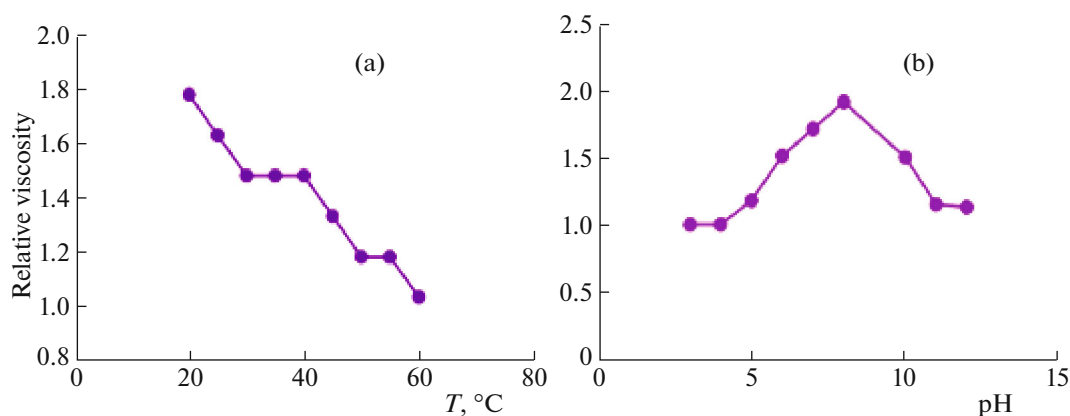


Fig. 10. (Color online) Typical plots for the effect (a) of temperature (at pH 6) and (b) of pH ($T = 30^\circ\text{C}$) on the relative viscosity for USG1.

the gel at $\text{pH} > 8$ was attributed to the aggregation of particle in basic microenvironment. These results also reflected that chemical (feeding) composition of the samples also influenced the microgel size.

Temperature and pH dependent changes in the flow viscosity of microgel solutions. To get more insight into the nature of volume phase changes and sol–gel behavior with variation in temperature and/or pH of solution, relative viscosity of microgel (5% solution of microgels) in aqueous media was also studied. Figure 10 showed the effect of temperature at constant pH (pH 6) and influence of pH at given temperature ($T = 30^\circ\text{C}$) on the relative viscosity of USG1. It was observed that viscosity decreased with increasing the solution temperature; however, the variation was not smoother but an irregular one. In the temperature range of $15\text{--}30^\circ\text{C}$, viscosity was decreasing, which became somewhat constant up to 40°C and then a continuous decrease was observed with temperature. This behavior was due to the temperature sensitivity and LCST of NIPAAm component of the gels, which is discussed in earlier sections. The temperature alters the hydrophilic/hydrophobic interaction of the gel. The other samples showed a similar trend except that the sample having a higher NIPAAm ratio (USG3) showed relatively large value of viscosity.

Figure 10b indicated the variation of relative viscosity as a function of solution pH, which again reflected the pH sensitivity of the gel was due to the presence of acrylic acid (AAc) co-monomer in the microgels network. The results depicted that with increase in pH the microgel particles indicated a continuous volume change in three stages. In the first stage the microgels viscosity remained constant (until pH 5) when the pH values were below the $\text{p}K_a$ value of AAc. In the second stage AAc groups deprotonated and ionized above the $\text{p}K_a$ value of AAc. This deprotonating led to swelling of microgels because of electrostatic repulsions among the negatively charged carboxylate units. All the AAc groups might be ionized at

pH value more than 8 and the hydrophilicity of microgels increased. Under these conditions the microgels grabbed large amount of water as well as increased their hydrodynamic diameter of microgel (LLS results) and same for the viscosity. Similarly, at $\text{pH} > 9$, the viscosity dropped again; this is due to the aggregation of the gel particles which could not pass through the capillary tube of viscometer and the flow was assigned to solvent dominant mixture.

Partial Specific Volume Study

Different physicochemical parameters were used to understand the solution behavior of different microgels, among those the partial molar specific volume (\bar{v}) could also be helpful to detect the solute–solute and solvent–solute interactions. It is important to remind here that the partial specific volume of a solute reflects the change in total volume dV per unit mass at constant pressure p and temperature T . Solution densities were measured for all samples and plotted versus solution concentration according to $\{\rho_{\text{soln}} = \rho_{\text{solv}} + (\bar{v}\rho_{\text{solv}})C\}$ [40]. Accordingly, the values of \bar{v} were obtained from the slope of the graphs (Fig. 11) using the approach $\{\bar{v} = \text{slope} \times 100 / \text{solvent density}\}$. A typical plot of density versus solution concentration for sample 2 was presented in Fig. 8, while other samples also show similar trend (figures not shown here). The resultant value of a specific volume of sample 1, 2, and 3 were found to be 2.49, 9.47, and 3.53 mL/g respectively. The difference in the values was linked to the difference in feeding/chemical composition of these samples. The higher value of partial specific volume (9.47 mL/g) for sample 2 was due to the higher ratio of acrylic acid (AAc) compared to other samples. Acrylic acid showed hydrophilic character and the hydrophilic interaction between gel particles enhanced the liquid like behavior for the gel which in turn increased the partial specific volume of particles.

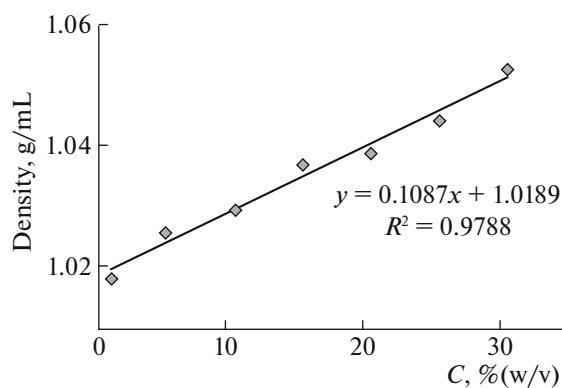


Fig. 11. Variation of solution density with concentration for USG2 at $T = 30^{\circ}\text{C}$.

Likewise, relatively higher value of \bar{v} for sample 3 as compared to sample 1 is due to more amount of hydrophilic NIPAAm in sample 3.

CONCLUSIONS

BMC-PNIPAAm-PAAC based polymer microgels with stimuli-responsive properties were successfully synthesized. The volume phase transition, swelling/de-swelling properties, rheological behavior, and optical properties of different compositions of BMC-PNIPAAm-PAAC microgels had been studied in aqueous medium under various experimental conditions. Rheological studies confirmed the volume phase transitions and temperature induced sol-gel behavior of the microgels. The shear stress and gel viscosity was measured at various shear rates and at different temperatures. Decrease in viscosity was observed by increasing shear rate. Viscous modulus (G''), storage modulus (G'), and gel deformation at various frequencies were also investigated. For all microgels samples, a transition from sol-to-gel behavior with temperature beyond 45°C and when $\text{pH} > 9$ was also noted. The swelling/de-swelling characteristics of the gels in terms of the relative viscosity and hydrodynamic size were also studied at different pH and temperature. Results revealed that the swelling/de-swelling behavior were found to depend on the lower critical solution temperature of NIPAAm and upper critical solution temperature of acrylic acid moieties. After a comprehensive investigation, it can be concluded that the physicochemical parameters were not only affected with fluctuating the chemical composition of microgels but also with the temperature/pH of the medium. Finally, the present work indicated that these responsive microgels with adjustable properties promise significant potential uses in the biomedical and chemical fields.

REFERENCES

1. Y. Zhang, H. Liu, and Y. Fang, *Chin. J. Chem.* **29**, 33 (2011).
2. S. Freiberg and X. Zhu, *Int. J. Pharm.* **282**, 1 (2004).
3. L. Zhang, F. X. Gu, J. M. Chan, A. Z. Wang, R. S. Langer, and O. C. Farokhzad, *Clin. Pharmacol. Ther.* **83**, 761 (2008).
4. R. A. A. Muzzarelli, P. Morganti, G. R. Morganti, P. Palombo, M. Palombo, G. Biagini, and M. M. C. Muzzarelli, *Carbohydr. Polym.* **70**, 274 (2007).
5. T. A. Sonia and C. P. Sharma, *Adv. Polym. Sci.* **243**, 23 (2011).
6. J. Kim, S. Nayak, and L. A. Lyon, *J. Am. Chem. Soc.* **127**, 9588 (2005).
7. D. E. Bergbreiter, B. L. Case, Y. S. Liu, and J. W. Caraway, *Macromolecules* **31**, 6053 (1998).
8. J. Kim, M. J. Serpe, and L. A. Lyon, *J. Am. Chem. Soc.* **126**, 9512 (2004).
9. K. Nagase, M. Kumazaki, H. Kanazawa, J. Kobayashi, A. Kikuchi, Y. Akiyama, M. Annaka, and T. Okano, *ACS Appl. Mater. Interface* **2**, 1247 (2010).
10. G. E. Morris, B. Vincent, and M. J. Snowden, *J. Colloid Interface Sci.* **190**, 198 (1997).
11. Z. H. Farooqi, A. Khan, and M. Siddiq, *Polym. Int.* **60**, 1481 (2011).
12. S. Juodkazis, N. Mukai, R. Wakaki, A. Yamaguchi, S. Matsuo, and H. Misawa, *Nature (London, U.K.)* **408**, 178 (2000).
13. O. A. Raitman, E. Katz, I. Willner, V. I. Chegel, and G. V. Popova, *Angew. Chem. Int. Ed.* **40**, 3649 (2001).
14. S. V. Ghugare, P. Mozetic, and G. Paradossi, *Biomacromolecules* **10**, 1589 (2009).
15. C. Chang, M. He, J. Zhou, and L. Zhang, *Macromolecules* **44**, 1642 (2011).
16. M. S. Nazir, B. A. Wahjoedi, A. W. Yusof, and M. A. Abdullah, *BioResources* **8**, 2161 (2013).
17. G. Cantero, A. Arbelaiz, R. Llano-Ponte, and I. Mondragonet, *Compos. Sci. Technol.* **63**, 1247 (2003).
18. H. M. Akil, L. W. Cheng Z. A. M. Ishak, A. A. Bakar, and M. A. A. Rahman, *Compos. Sci. Technol.* **69**, 1942 (2009).
19. L. Verestiuc, C. Ivanov, E. Barbu, and J. Tsibouklis, *Int. J. Pharm.* **269**, 185 (2004).
20. N. Sanson and J. Rieger, *Polym. Chem.* **1**, 965 (2010).
21. Z. H. Farooqi, R. Begum, K. Naseem, U. Rubab, M. Usman, A. Khan, and A. Ijaz, *Russ. J. Phys. Chem. A* **90**, 2600 (2016).
22. R. Hernández and C. Mijangos, *Macromol. Rapid Commun.* **30**, 176 (2009).
23. A. Khan, M. B. H. Othman, B. P. Chang, and H. M. Akil, *Iran. Polym. J.* **24**, 317 (2015).
24. M. R. Aguilar, C. Elvira, A. Gallardo, B. Vázquez, and J. Román, in *Topics in Tissue Engineering*, Ed. by N. Ashammakhi, R. L. Reis, and E. Chiellini (Univ. of Oulu, Finland, 2007), Vol. 3, p. 2.
25. H. Y. Shi, L. Zhang, Y. Q. Ma, and J. Z. Yi, *J. Macromol. Sci., A* **44**, 1109 (2007).

26. A. S. Singha and A. K. Rana, *Bull. Mater. Sci.* **35**, 1099 (2012).
27. S. Köhler and T. Heinze, *Macromol. Biosci.* **7**, 307 (2007).
28. A. Khan, M. B. H. Othman, K. A. Razak, and H. M. Akil, *J. Polym. Res.* **20**, 273 (2013).
29. R. P. Dumitriu, G. R. Mitchell, and C. Vasile, *Polym. Int.* **60**, 1398 (2011).
30. U. G. Spizzirri, F. Iemma, F. Puoci, F. Xue, W. Gao, G. Cirillo, M. Curcio, O. I. Parisi, and N. Picci, *Polym. Adv. Technol.* **22**, 1705 (2011).
31. J. P. Chen and T. H. Cheng, *Polymer* **50**, 107 (2009).
32. Z. Li, J. Shen, H. Ma, X. Lu, M. Shi, N. Li, and N. M. Ye, *Mater. Sci. Eng. C* **33**, 1951 (2013).
33. A. Y. Malkin, A. Semakov, and V. Kulichikhin, *Adv. Colloid Interface* **157**, 75 (2010).
34. A. Chetty, J. Kovács, Z. Sulyok, A. Mészáros, J. Fekete, A. Domján, A. Szilágyi, and V. Vargha, *Express Polym. Lett.* **7**, 95 (2013).
35. M. Fathi, A. A. Entezami, and R. Pashaei-Asl, *J. Polym. Res.* **20**, 125 (2013).
36. D. Missirlis, J. Hubbell, and N. Tirelli, *Soft Matter* **2**, 1067 (2006).
37. F. Zeng, X. Zheng, and Z. Tong, *Polymer* **39**, 1249 (1998).
38. Z. Yang, B. Cao, J. Zhu, J. Shen, J. Li, S. Guo, and Y. Wang, *Polym. Compos.* **33**, 1432 (2012).
39. M. H. Ghatee, M. Zare, F. Moosavi, and A. R. Zolghadr, *J. Chem. Eng. Data* **55**, 3084 (2010).
40. A. Khan and M. Siddiq, *J. Appl. Polym. Sci.* **118**, 3324 (2010).